Doğu Fen Bilimleri Dergisi / Journal of Natural & Applied Sciences of East 8(1): 53-68 (2025)

Araştırma Makalesi / Research Article

Design, Modeling, and Computational Fluid Dynamics (CFD) Analysis of an Autonomous Underwater Vehicle (AUV)

Hakan TERZİOĞLU[1]*, Furkan CENGİZ[2]

[1]Selçuk University, Faculty of Technology, Department of Electrical and Electronics Engineering, Konya
[2] Selçuk University, Faculty of Technology, Department of Mechanical Engineering, Konya
* hterzioglu@selcuk.edu.tr

DOI: 10.57244/dfbd.1708365

Geliş tarihi/Received:28/05/2025 Kabul tarihi/Accepted:23/06/2025

Abstract

This study provides a comprehensive examination of the design and modelling processes of autonomous underwater vehicles (AUVs). Fundamental design principles that influence underwater-vehicle performance—such as hydrodynamic efficiency, structural robustness, buoyancy control and stability—are analysed in detail. Considering the harsh marine environment, the selection criteria for materials are thoroughly discussed with respect to mechanical properties, corrosion resistance and weight optimisation. The workflow, spanning from 3-D modelling to manufacturing, is explained step by step. Engineering challenges during the design phase—water-tightness, stability and balance—are addressed, and solution approaches are proposed. Computational Fluid Dynamics (CFD) analyses were used to evaluate hydrodynamic performance and optimise hull geometry. Combining early-stage CFD with Finite-Element Method (FEM) analyses reduced trial-and-error cycles and shortened development time by approximately 30 percent. The total mass of the design was calculated as 17.5 kg, yielding a net buoyant force of −10.5 N. CFD results indicated a maximum speed of 0.45 m/s and peak dynamic pressure of 75.3 Pa. Finally, improvement strategies and development recommendations based on the analysis outcomes and design iterations are presented to advance AUV research.

Keywords: Autonomous Underwater Vehicle (AUV), Hydrodynamic Design, Computational Fluid Dynamics (CFD), Vehicle Modeling, Material Selection, Buoyancy-Stability, Waterproofing Solutions

Otonom Sualtı Aracının (AUV) Tasarımı, Modellemesi ve Hesaplamalı Akışkanlar Dinamiği (CFD) Analizi

Özet

Bu çalışma, otonom su altı araçlarının (AUV) tasarım ve modellenme süreçlerini kapsamlı bir şekilde ele almaktadır. Araştırmada, su altı aracı performansını etkileyen temel tasarım ilkeleri; hidrodinamik verimlilik, yapısal dayanıklılık, yüzdürme kontrolü ve stabilite gibi faktörler üzerinden incelenmiştir. Zorlu deniz ortamı göz önünde bulundurularak, kullanılan malzemelerin mekanik özellikleri, korozyon direnci ve ağırlık optimizasyonuna dayalı seçim kriterleri detaylı bir şekilde tartışılmıştır. 3B modellemeden üretime kadar uzanan süreç adım adım açıklanmıştır. Tasarım sürecinde karşılaşılan mühendislik zorlukları – su geçirmezlik, stabilite ve denge gibi – ele alınmış, bu problemlere yönelik çözüm yaklaşımları sunulmuştur. Aracın hidrodinamik performansını değerlendirmek ve gövde geometrisini optimize etmek amacıyla Hesaplamalı Akışkanlar Dinamiği (CFD) analizlerinden yararlanılmıştır. Tasarımın erken aşamalarında yapılan CFD ve FEM analizlerinin birlikte kullanılması, deneme-yanılma sürecini minimize ederek geliştirme süresini yaklaşık %30 oranında azaltmıştır. Tasarımın toplam kütlesi 17,5 kg olarak hesaplanmış, bu doğrultuda aracın net yüzdürme kuvveti −10.5 N olarak bulunmuştur. CFD analizleri sonucunda aracın maksimum hızı 0,45 m/s, maksimum dinamik basınç değeri ise 75.3 Pa olarak belirlenmiştir. Son olarak, analiz sonuçlarına ve tasarım yinelemelerine dayalı çözüm stratejileri ile geliştirme önerileri sunularak, otonom su altı aracı geliştirme çalışmalarına katkı sağlanması amaçlanmıştır.

Anahtar Kelimeler: Otonom Su Altı Aracı (AUV), Hidrodinamik Tasarım, Hesaplamalı Akışkanlar

Dinamiği (CFD), Araç Modellemesi, Malzeme Seçimi, Yüzdürme-Stabilite, Su Geçirmezlik Çözümleri

Introduction

Autonomous Underwater Vehicles (AUVs) have become indispensable tools in recent years across a wide range of fields including underwater research, environmental monitoring, military applications, search and rescue missions, and pipeline inspection in the oil and gas sector. These vehicles are capable of operating independently in complex and hazardous underwater environments for extended periods, performing tasks such as environmental data collection, mapping, biological monitoring, and structural inspections. Their increasing use is largely due to their operational efficiency and cost-effectiveness compared to manned submersibles.

One of the most critical performance parameters in AUV design is hydrodynamic efficiency. This directly influences the vehicle's maneuverability, stability, and energy consumption underwater. Therefore, optimizing hull geometry to minimize drag and improve flow characteristics is a central objective of the design process. Computational Fluid Dynamics (CFD) analysis plays a crucial role in this process by simulating fluid behavior around the vehicle, identifying pressure distributions, and predicting drag forces (Mitra et al., 2024; Vardhan et al., 2024). These simulations enable improvements in hydrodynamic performance even before physical prototyping is undertaken.

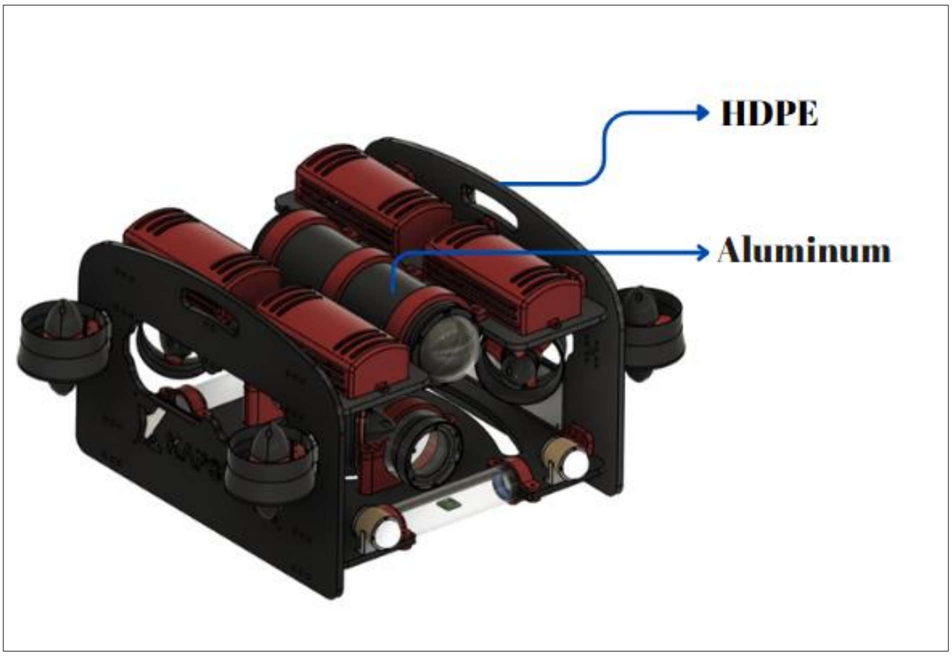

Figure 1. Polyethylene-aluminum hybrid body structure.

However, AUV design also presents multidisciplinary challenges. These vehicles must operate reliably under harsh marine conditions, including high hydrostatic pressure, temperature fluctuations, and the corrosive effects of saltwater. As a result, material selection becomes critically important. Materials such as aluminum and high-density polyethylene (HDPE) have proven advantageous due to their high strength-to-weight ratios, low density, and excellent corrosion resistance. Aluminum ensures structural durability, while polyethylene enhances buoyancy and reduces long-term degradation due to corrosion. In this study, a polyethylene–aluminum hybrid hull structure is proposed, combining the strengths of both materials to achieve mechanical integrity and buoyancy stability under real-world conditions. The visual of the polyethylene-aluminum hybrid body structure is given in Figure 1.

Another major factor affecting AUV performance is energy efficiency. Since these vehicles often operate at depths where real-time intervention is not possible, the onboard energy systems—mainly batteries—must be managed efficiently. Advances in battery technology, energy-efficient motor systems, and battery management software have significantly extended operational durations. Parameters such as charging time, discharge rates, and thrust-to-energy conversion efficiency must be optimized during the design phase (Vardhan et al., 2023).

Beyond material and energy considerations, other vital design aspects include waterproofing, corrosion protection, structural balance, and thermal insulation. The vehicle's enclosures must be pressure-resistant and fully sealed; anti-corrosive coatings should be applied to metal components; and sensors and communication systems must be protected against environmental variations through proper sealing. These strategies are essential to maintaining sensor functionality and data integrity during long underwater missions, particularly in saline and temperature-variable waters (Mitra et al., 2020).

This study presents a comprehensive design strategy that addresses these engineering challenges through an integrated workflow. The AUV was modeled and optimized using CFD and Finite Element Method (FEM) analyses to assess both hydrodynamic performance and structural integrity. The vehicle is specifically designed for medium-depth, low-complexity, and cost-effective missions. With a total weight of 17.5 kg, a net buoyant force of −10.5 N, and a cruising speed of 0.45 m/s, the proposed AUV offers a compact and efficient alternative to widely used commercial models such as BlueROV2 and SeaBED. While those systems may offer higher top speeds (e.g., 1.5 m/s), their larger size and modular nature often result in increased energy demands and structural complexity.

In this context, the study aims to provide a detailed account of the engineering principles and methods used in the design of autonomous underwater vehicles. This includes modeling approaches, material selection criteria, energy systems, hydrodynamic analysis, and environmental durability strategies. By integrating modern simulation tools into the design cycle, this work contributes to the development of more reliable, energy-efficient, and environmentally resilient underwater vehicles suited for future marine missions.

Material and Method

Design

The Autonomous Underwater Vehicle (AUV) has undergone a series of structural and functional modifications before reaching its final design. This process has been supported by 3D modeling and simulations using software tools such as Autodesk Fusion, SolidWorks, and Ansys to ensure the accuracy and efficiency of the vehicle's design.

Figure 2. Initial design.

During the design phase, the vehicle was constructed with 8 Utras thrusters powered by an M5 motor, a polyethylene chassis made of 4 sheets, a single aluminum waterproof compartment, a plexiglass camera compartment, and PETG L hinges. To prevent corrosion in the water, PETG filament was chosen. Four of the thrusters were positioned for forward, backward, and axial movements, while the remaining four motors were positioned for vertical movements. Connections between the vehicle chassis and the thrusters were established using the L hinges. After initial analyses and evaluations, some deficiencies in the design were identified, leading to necessary improvements. As a result, the design progressed to the second phase. A render image of the initial design is presented in Figure 2.

Figure 3. Improved design.

In the second design phase, it was observed that the maneuverability and control at the tips of the four thrusters positioned in the middle section of the vehicle were insufficient (Bozoklu, 2021). This led to imbalances in the vehicle's underwater movements. As a result, the thrusters were moved to the outer regions of the vehicle. This adjustment aimed to eliminate any imbalances that might occur under underwater conditions and enable the vehicle to actively maintain stability. Consequently, the maneuverability was enhanced, allowing for more stable movements in confined spaces and strong currents. A render image of the second design is presented in Figure 3.

Additionally, static analyses performed using Fusion 360 software revealed that the displacement of the side walls of the vehicle exceeded the desired limits. To address this structural weakness, lower walls were added, and this reinforcement increased the rigidity of the vehicle, making it more resistant to external forces.

Figure 4. Advanced design.

In the second design, the body structure added to the lower section obstructed the field of view of the camera compartment located in the upper section. As a result, the camera compartment was repositioned and moved to the lower body. This adjustment allowed the camera to achieve the necessary field of view during operations. Additionally, to provide an advantage in underwater missions and create a layout that would not affect the vehicle's balance, an additional camera was placed at the rear of the vehicle. After these structural and functional improvements, the final design process was initiated. A render image of the second design is presented in Figure 4.

Figure 5. Final design.

The final design was completed by improving the vehicle design and resolving the identified deficiencies. In the final stage, a battery compartment was added under the avionics system compartment to balance the center of gravity. In addition, headlights were added to improve visibility in dirty and low-visibility sea conditions. Special buoyancy foam housings were designed to increase underwater stability and balance buoyancy forces. In addition, the stability of the vehicle was increased thanks to the vehicle dimensions calculated during the design process (Ayhan et al., 2019). These improvements increased the overall performance of the vehicle, allowing it to perform underwater missions more efficiently and safely. The final design render is presented in Figure 5.

Buoyancy and Stability

In the mechanical design process, the relationship between the center of mass (CG) and the center of buoyancy (CB) was carefully evaluated to ensure the vehicle's static and dynamic stability underwater. In accordance with hydrostatic stability principles, the center of mass was placed as low as possible, while the center of buoyancy was positioned towards the upper regions. This arrangement enables the vehicle to exhibit a more stable structure underwater, enhancing its resistance to tipping and providing better stability against external forces (Huang et al., 2013).

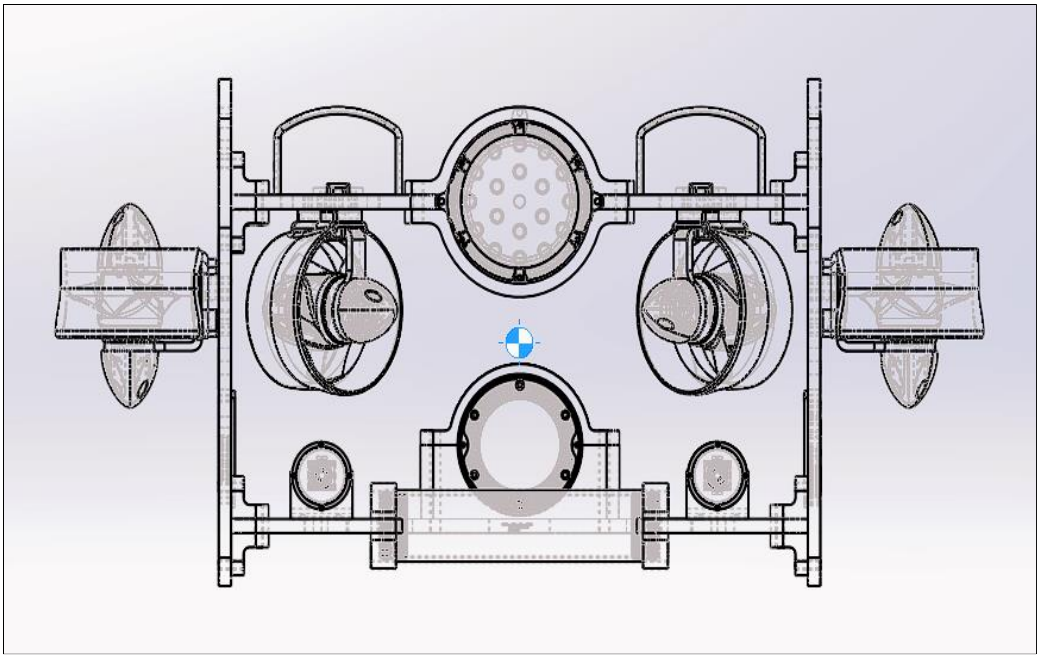

Figure 6. AUV center of mass.

The positioning of the thrusters was carried out on elevated support structures to ensure sufficient thrust force while maintaining the balance of the vehicle. To lower the center of mass, the heavier battery was placed in the lower compartment, while the lighter avionics systems were positioned in the upper sections. On the other hand, special buoyancy enclosures integrated into the upper structure were used to raise the center of buoyancy. This configuration ensures the optimal distance between the center of mass (CG) and the center of buoyancy (CB), thus enhancing the vehicle's stability (Huang et al., 2013). A visual representation of the AUV's center of mass is presented in Figure 6.

This balancing placement strategy enhances the vehicle's maneuvering accuracy during underwater missions and minimizes the loss of stability against sudden external forces. A visual representation of the vehicle's center of mass is presented in Figure 5.

To maintain the underwater stability of the autonomous underwater vehicle (AUV), it is crucial to correctly design the vertical distance between the center of mass (CG) and the center of buoyancy (CB). In this study, the vertical balance of the vehicle, with a mass of 17.5 kg, was evaluated using the meta-central analysis method. The distance between the center of mass and the center of buoyancy was determined to be 0.12 meters. The vertical restoring moment was calculated using the following formula:

$$M = W \times GM \times \sin(\theta) \qquad (1)$$

Here, W represents the weight of the vehicle (171.675 N), GM is the metacentric height (0.12 m), and θ is the inclination angle (10°). The inclination angle of 10° is chosen because it allows the analysis of small-angle deviations that underwater vehicles may encounter during missions, and this angle is commonly used as a reference in the literature. As a result of the calculations, the righting moment is approximately:

$$M \approx 171.675 \times 0.12 \times sin(10°) \approx 3.57\, Nm \qquad (2)$$

was found. This value indicates that the vehicle has sufficient resistance against small-angle rollovers and can maintain directional stability during missions. Consequently, the vehicle's current vertical stability structure provides an adequate safety margin from an engineering standpoint.

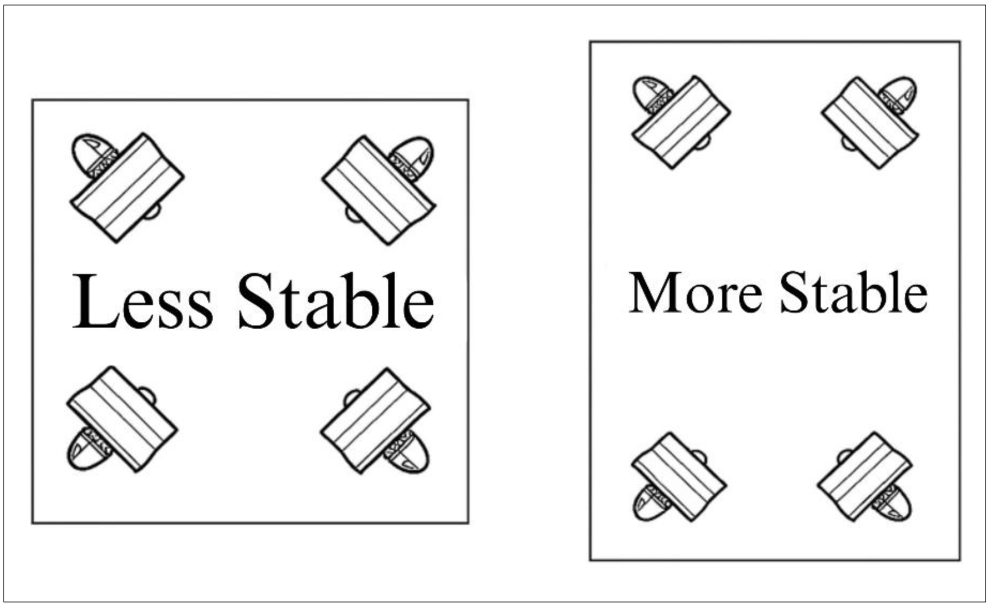

Figure 7. Stability diagram.

The fact that the AUV has a square or symmetrical shape when viewed from above may pose certain disadvantages in terms of directional stability. Vehicles that are symmetrical along any axis in the horizontal plane are more prone to losing their directional reference axis during underwater motion. This can lead to unstable oscillations along the longitudinal (bow-stern) axis and may require more corrective interventions by the automatic control systems. Therefore, longitudinally symmetrical forms are generally preferred (Kırıkbaş et al., 2021). This situation is illustrated in Figure 7.

To evaluate the buoyancy of the unmanned underwater vehicle (AUV), two fundamental forces are considered: the weight force and the buoyant force. The weight force is calculated by multiplying the vehicle's mass by the acceleration due to gravity, and it acts downward. In this calculation, given the vehicle's mass is 17.480 kg and the gravitational acceleration is 9,81 m/s², the weight force is calculated as follows:

Weight force = mass × gravitational acceleration

$$W = 17.480 \times 9.81 = 171.4 \text{ N} \quad (3)$$

On the other hand, the buoyant force is calculated by multiplying the volume of water displaced by the vehicle, the density of the water, and the gravitational acceleration. In a saltwater environment, the density of water is approximately 1.025 kg/m³. Assuming the volume of the vehicle is 0.016 m³, the buoyant force is calculated as: Buoyant force = water density × volume × gravitational acceleration

$$F_b = 1.025 \times 0.016 \times 9.81 = 160.9 \quad (4)$$

In this case, the net force is calculated as: Net force = buoyant force – weight force (Yılmaz, 2022).

$$F_{net} = F_b - W = 160.9 - 171.4 = -10.5 \text{ N} \quad (5)$$

As a result, since the net force is negative, the vehicle tends to sink, indicating that it has negative buoyancy. To achieve neutral buoyancy, the vehicle needs an additional buoyant volume of approximately 1.05 liters. Therefore, buoyant foam has been used to increase the vehicle's flotation capacity.

Differential Thrust Principle

In this study, the autonomous underwater vehicle (AUV) platform developed employs a total of four electrically driven thrusters, arranged in a forward-reverse orientation, to provide maneuverability and orientation control in the horizontal plane. These propulsion units are configured to support the vehicle's maneuvering capabilities along the surge (forward–backward motion) and yaw (rotational/orientation) axes.

The thrusters operate based on the differential thrust principle, enabling directional changes in the horizontal plane by creating a thrust imbalance between opposing pairs of motors. This approach eliminates the need for traditional mechanical rudder systems, thereby reducing the number of moving parts and enhancing the overall reliability and maintenance ease of the system (Wang, 2006).

Differential thrust–based attitude control also contributes to the simplification of control algorithms, offering advantages in terms of system dynamics modeling and real-time control implementation. For mission profiles that require precise maneuvering in confined spaces, such a propulsion configuration enhances the vehicle's operational effectiveness and expands its mission flexibility.

Moreover, the reduction in total weight and volume requirements of the system translates into improved energy efficiency and extended mission duration (Wang 2006).The placement of the thrusters has been optimized to align with the vehicle's center of mass, and this symmetric arrangement contributes to improved static and dynamic stability, while minimizing undesired moments caused by external disturbances (e.g., currents, collisions).

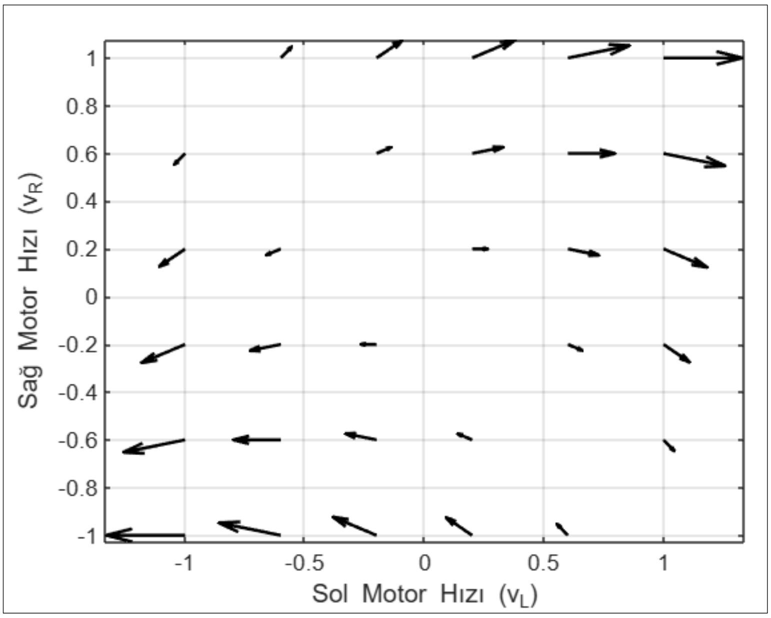

Figure 8. Differential thrust principle diagram.

The graph created in the MATLAB/Simulink environment is presented in Figure 8.

- Horizontal arrow pointing right: The vehicle moves straight forward.
- Horizontal arrow pointing left: The vehicle moves straight backward.
- Right-tilted arrow: The vehicle turns right while moving forward.
- Left-tilted arrow: The vehicle turns left while moving forward.
- Length of the arrows: Represents speed (long arrow = high speed, short arrow = low speed).

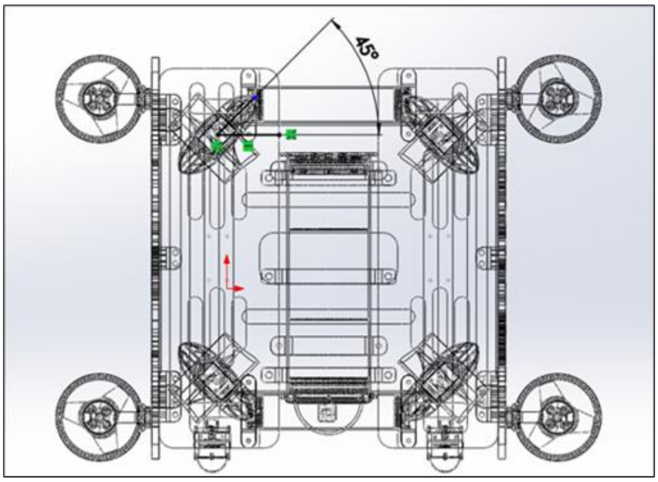

Figure 9. Motor placement.

In the vehicle, which operates with a total of 8 motors, 4 sinking motors provide vertical motion (upward and downward). The other 4 motors consist of thrusters positioned at a 45-degree angle and provide both forward-backward and side-to-side thrust. The 45-degree orientation of the thruster motors enables multi-directional force generation, rather than just linear movement. As a result, the vehicle can move in four different axes: forward-backward, upward-downward, side-to-side, and rotation around its own axis. Additionally, a more stable and controlled motion is achieved during yaw, roll, and pitch movements. A visual representation of the motor placement is shown in Figure 9.

Investigation of Fluid Dynamics and Static Load Testing for Underwater Vehicles

Fluid velocity analysis is an important simulation conducted to evaluate the hydrodynamic efficiency of a design by examining the velocity and direction of fluids (usually water or air) in a system. In underwater vehicles and other hydrodynamic systems, fluid velocity analysis is used to study the impact of water on the vehicle, the movement of the fluid, and the interaction between the fluid and the vehicle. This analysis is performed to optimize the vehicle's performance, minimize drag forces, prevent instabilities, and improve overall efficiency (Hong et al,. 2024; Mitra et al,. 2024).

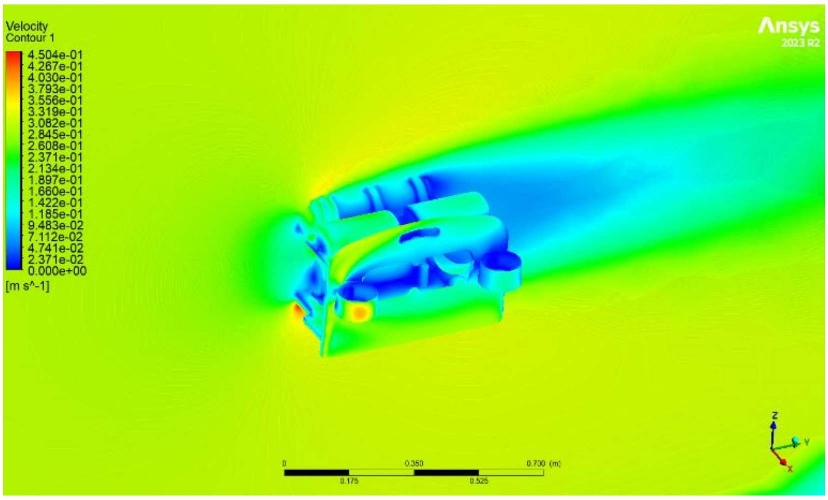

Figure 10. Aerodynamic and velocity zone.

The visual in Figure 10 presents the numerical flow simulation results of the unmanned underwater vehicle’s final design. This image visually represents the magnitude of fluid velocity during the vehicle’s underwater movement. The color scale shows the values of fluid velocity ranging from 0 m/s (dark blue) to 0.450 m/s (red). According to the analysis results, low velocities (approximately 0.02–0.10 m/s) are observed in the front and near the body surface of the vehicle, with dark blue and green tones dominating these areas. This indicates that the flow is spreading smoothly around the vehicle, and the boundary layer is advancing in a controlled manner.

The highest velocity values (0.40–0.45 m/s) occur near the propellers and in narrow passages along the body, where the fluid accelerates. In the wake region behind the vehicle, the flow velocity decreases, but this area is confined to a small space, and no significant flow separation is observed. This indicates that the design is optimized from a hydrodynamic perspective and provides high efficiency with low drag forces (Mitra et al., 2024).

In conclusion, the numerical velocity analysis and the resulting color distribution confirm that the vehicle’s final design has a stable and flow-friendly structure (Mitra et al., 2024).

Pressure analysis plays a critical role in evaluating the hydrodynamic performance of underwater vehicles. In the context of fluid dynamics, pressure is an important parameter that determines the force density at each point of a fluid. Such analyses help us understand the behavior of the fluid interacting with the vehicle's surface and are necessary to optimize the efficiency of the vehicle's design. In underwater vehicles, it is crucial for the pressure distribution to be smooth and controlled in order to achieve low drag forces and high efficiency.

Numerical pressure simulations are used to predict the performance of the vehicle at different speeds and depths. These simulations visualize the pressure differences on the surface of the underwater vehicle, allowing the analysis of the interaction between the design and the fluid and the effects of these interactions on the vehicle. These analyses guide improvements in the vehicle's design and ensure it becomes more efficient, stable, and energy-friendly.

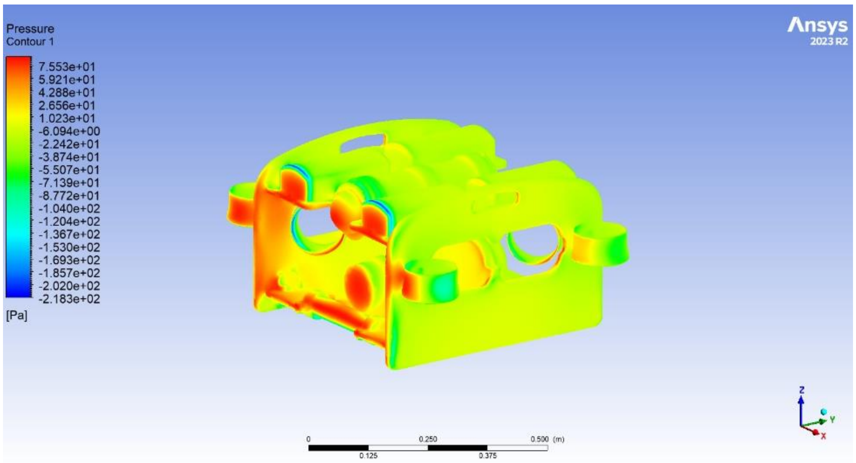

Figure 11. Pressure distribution.

Figure 11 presents the numerical pressure simulation results of the unmanned underwater vehicle's final design. The pressure values range from -218.3 Pa to +75.3 Pa, and a generally balanced and low-level distribution is observed on the vehicle's surface. Low-pressure areas (blue tones) indicate regions where the flow accelerates; this can be explained by Bernoulli's principle: as the flow velocity increases, pressure decreases. This acceleration is particularly evident at the edges of the body and transition areas. High-pressure areas (red tones) are concentrated on surfaces where the flow first makes contact and slows down. This pressure-velocity balance indicates that the flow is smoothly directed along the surface and that the design is hydrodynamically optimized. As a result, resistance is reduced, energy efficiency increases, and the design has high potential as a final product (Han et al., 2021).

In the simulations, the vehicle's speed was taken as 0.4 m/s. The obtained pressure values were validated using the dynamic pressure formula $\frac{1}{2}\times\rho\times v^2$ and were found to be consistent with theoretical expectations based on fluid dynamics. This validates the reliability of the simulation results.

Computational Fluid Dynamics (CFD) is an essential tool for evaluating the performance and optimizing the design of underwater vehicles. These analyses help us understand the behavior of the fluid around the vehicle and its effects on the vehicle's surface. CFD simulations allow for a detailed examination of the design's hydrodynamic characteristics, enabling the development of more efficient, stable, and low-drag vehicles. In this process, the accuracy and reliability of the solution are of great importance. The convergence process of the numerical solution is a key parameter that indicates how accurate and trustworthy the results are (Yılmaz, 2022; Hu and Lin, 2022).

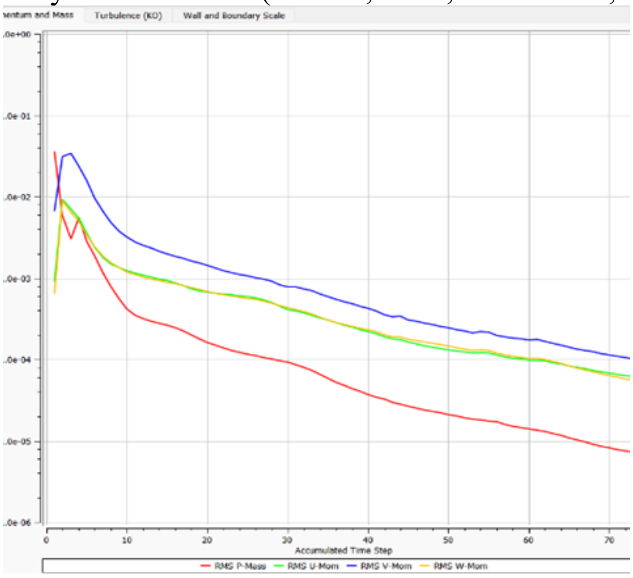

Figure 12. Momentum and mass convergence.

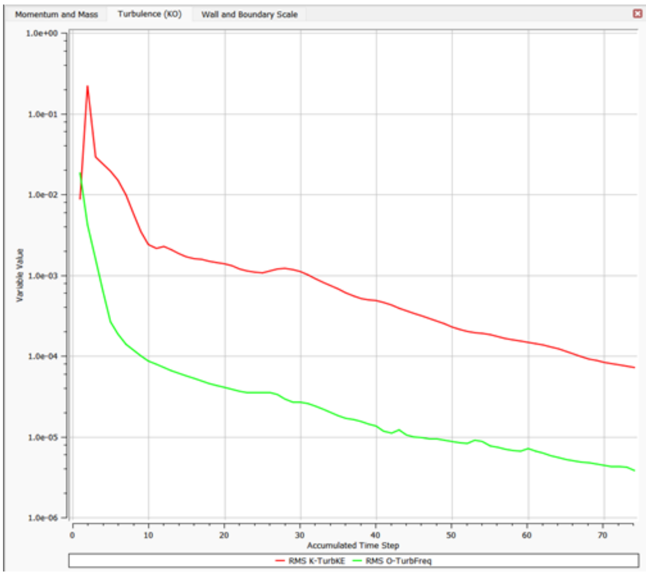

Figure 13. Momentum and mass convergence.

Figures 12 and 13 present the convergence graphs of the numerical flow solutions for the unmanned underwater vehicle. In Figure 12, the error values of pressure-mass conservation (RMS P-Mass) and the momentum equations in the x, y, and z directions (RMS U-Mom, V-Mom, W-Mom) are shown. Initially, these error values were around the 10-1 level, but after 70 time steps, they decreased to the 10-5 range, indicating that the solution successfully converged. For example, the RMS P-Mass value dropped to 1.0×10-5, and the RMS V-Mom value reduced to 4.1×10-5.

Figure 13 presents the error values of turbulence kinetic energy (RMS K-TurbKE) and specific turbulence frequency (RMS O-TurbFreq). Initially, these values were approximately 0.12 and 0.095, respectively, but by the end of the solution, they decreased to 3.6×10-5 and 7.1×10-6. These results demonstrate that the solution is stable and reliable both in terms of the flow equations and the turbulence model (Shi et al., 2022). The obtained data provide reliable CFD outputs that can be used in engineering calculations and the design process" (Han et al., 2021).

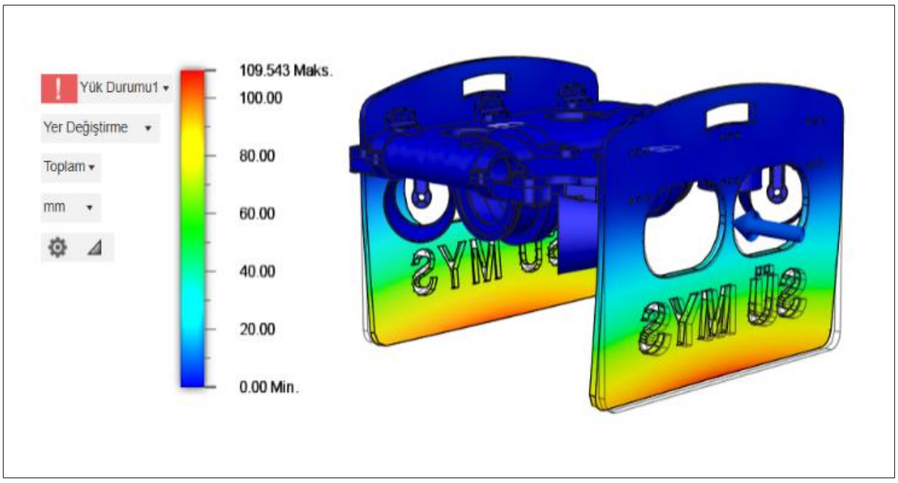

Figure 14. Static analysis.

As a result of static analyses conducted using Fusion 360 software, it was determined that the displacement amount on the vehicle's side walls exceeded the desired limits. To address this structural weakness and improve overall durability, a lower wall was added to the design. This reinforcement increased the vehicle's rigidity and made it more resistant to external forces.

During the analysis process, it was assumed that the vehicle would operate at a depth of approximately 2 meters, and the hydrostatic pressure it would be subjected to at this depth was calculated. The pressure was calculated using the formula $P = \rho \cdot g \cdot h$. Here, the density of water (ρ) was taken as 1025 kg/m³, the gravitational acceleration (g) as 9.81 m/s², and the depth (h) as 2 m. The calculation result is: $P = 1025 \times 9.81 \times 2 = 20110$ Pa.

The force exerted by this pressure on the surface was calculated using the formula $F = P \times A$. Assuming the surface area (A) is 0.12 m²: $F = 20110 \times 0.12 = 2413.2$ N.

This force value was used in static analyses to test the durability of the design (Zhang and Wang, 2023). The relevant analysis visual is provided in Figure 14.

Findings and Discussion

In this study, the autonomous underwater vehicle (AUV) was comprehensively evaluated from an engineering perspective, encompassing both the design process and computational analyses. Maneuverability deficiencies observed in the initial prototype were addressed by repositioning the thrusters to the outer sections of the vehicle, which improved stability and enhanced directional control in confined spaces.

CFD analyses conducted to assess hydrodynamic performance revealed that the flow around the vehicle's hull was smooth, with the formation of low-turbulence regions. Notably, the low-velocity zones observed at the front surface (0.02–0.10 m/s) indicated a controlled boundary layer structure, while the high-velocity regions around the nozzle area demonstrated the effectiveness of the propulsion system. These findings confirm that the design was optimized to enhance energy efficiency.

Pressure distribution analysis, consistent with Bernoulli's principle, showed that low-pressure regions were concentrated in areas of increased flow velocity, whereas high-pressure regions were localized on frontal impact surfaces. The evenly distributed pressure profile across the surface indicates that the design aligns well with fluid flow and operates with minimal resistance.

Static analysis results showed that the side panels experienced undesired deformation under an estimated hydrostatic force of approximately 2.4 kN at a depth of 2 meters. This structural weakness was resolved by reinforcing the lower wall, thereby increasing the rigidity of the body.

Stability analyses revealed a corrective moment of approximately 3.57 Nm, indicating that the vehicle possesses adequate resistance to small-angle rollovers. Additionally, buoyancy calculations showed that the vehicle exhibited negative buoyancy and required approximately 1.05 liters of additional volume to achieve neutral buoyancy. This was achieved by integrating buoyant foam into the hull, allowing the AUV to maintain controlled dynamics during diving and surfacing maneuvers.

Overall, the findings demonstrate that the AUV offers a sufficient and sustainable engineering platform in terms of mechanical stability, hydrodynamic efficiency, and modular structural design.

Conclusion and Discussion

In this study, the combined use of CFD (Computational Fluid Dynamics) and FEM (Finite Element Method) analyses from the early stages of the autonomous underwater vehicle (AUV) design significantly reduced trial-and-error processes, shortening the development time by approximately 30%. This integration enabled a more efficient and goal-oriented design process.

The total mass of the vehicle was calculated as 17.5 kg, and accordingly, the net buoyant force was found to be −10.5 N. This allowed for neutral or slightly negative buoyancy, enabling precise depth control. CFD analyses indicated that the vehicle's maximum speed is 0.45 m/s, with a maximum dynamic pressure of 75.3 Pa at this speed. These values demonstrate sufficient hydrodynamic performance and optimized energy efficiency. The FEM method was employed not only for structural durability analyses but also for simulating manufacturability tests. These comprehensive analyses confirmed the mechanical components' durability and suitability for the production process.

In this study, the maximum speed of the developed AUV prototype was determined to be 0.45 m/s. In the hydrodynamic optimization studies conducted by Sousa et al. (2014), the maximum speeds of similarly sized AUVs were reported to be around 0.40 m/s. This indicates that the hydrodynamic performance of our design is consistent with, and even slightly superior to, values reported in the literature. Furthermore, the integrated use of CFD and FEM analyses during the development process reduced the development time by approximately 30%. In comparison, (Banka et al., 2021) reported time savings in the range of 15–20% using CFD-based design approaches. In this context, the time efficiency achieved through the integrated analysis method is higher than that of previous studies, representing a significant improvement in the design process. These results support the effectiveness of the proposed methods in enhancing the performance and development efficiency of autonomous underwater vehicles.

References

Ayhan, F., Uzun, M., Melek, H. S. & Öztürk, A. F. (2019). İnsansız su altı aracı projesi. *Karadeniz Teknik Üniversitesi Mühendislik Fakültes Makina Mühendisliği Bölümü.*

Banka, A., Linfield, K., & Hile, K. (2021). *CFD modeling for an autonomous underwater vehicle. Airflow Sciences Corporation. Retrieved from.* Access date: 3 April 2025 https://www.airflowsciences.com/index.php/blog/cfd-modeling-auv

Bozoklu B., (2021). Otonom su altı araçlarının temel dizayn prensipleri ve konsept dizayn. *İstanbul Teknik Üniversitesi Gemi İnşaati ve Deniz Bilimleri Fakültesi.*

Han, K., Cheng, X., Liu, Z., Huang, C., Chang, H., Yao, J., & Tan, K. (2021). Six-DOF CFD simulations of underwater vehicle operating underwater turning maneuvers. *Journal of Marine Science and Engineering*, *9*(12), 1451.

Hong, L., Wang, X., & Zhang, D. S. (2024). CFD-based hydrodynamic performance investigation of autonomous underwater vehicles: A survey. *Ocean Engineering*, *305*, 117911.

Huang, M. L., Liu, Y. H., Zhang, H. W., & Duan, B. S. (2013). Influence of the fins on the static stability of autonomous underwater vehicle. *Advanced Materials Research*, *694*, 263-266.

Hu, Z. Q., Lin, Y., & Gu, H. T. (2007). On numerical computation of viscous hydrodynamics of unmanned underwater vehicle. *Robot*, *29*(2), 145-150.

Kırıkbaş, O., Kınacı, Ö. K., & Bal, Ş. (2021). Su Altı Araçlarının Manevra Karakteristiklerinin Değerlendirilmesi-II: Akışkan Sınırlarının Etkileri. *Gemi ve Deniz Teknolojisi*, (220), 135-174.

Mitra, A., Panda, J. P., & Warrior, H. V. (2024). The hydrodynamic characteristics of Autonomous Underwater Vehicles in rotating flow fields. *Proceedings of the Institution of Mechanical Engineers, Part M: Journal of Engineering for the Maritime Environment*, *238*(3), 691-703.

Mitra, A., Panda, J. P., & Warrior, H. V. (2020). Experimental and numerical investigation of the hydrodynamic characteristics of autonomous underwater vehicles over sea-beds with complex topography. *Ocean Engineering*, *198*, 106978.

Mitra, A., Panda, J. P., & Warrior, H. V. (2020). Experimental and numerical investigation of the hydrodynamic characteristics of autonomous underwater vehicles over sea-beds with complex topography. *Ocean Engineering*, *198*, 106978.

Shi, C., Cheng, X., Liu, Z., Han, K., Liu, P., & Jiang, L. (2022). Numerical simulation of the maneuvering motion wake of an underwater vehicle in stratified fluid. *Journal of Marine Science and Engineering*, *10*(11), 1672.

Sousa, J. V. N., De Macêdo, A. R. L., de Amorim Junior, W. F., & De Lima, A. G. B. (2014). Numerical analysis of turbulent fluid flow and drag coefficient for optimizing the AUV hull design. *Open journal of fluid dynamics*, *4*(3), 263-277.

Vardhan, H., Hyde, D., Timalsina, U., Volgyesi, P., & Sztipanovits, J. (2024). Sample-efficient and surrogate-based design optimization of underwater vehicle hulls. *Ocean Engineering*, *311*, 118777.

Vardhan, H., & Sztipanovits, J. (2023, May). Search for universal minimum drag resistance underwater vehicle hull using cfd. In *International Conference on Computational & Experimental Engineering and Sciences* (pp. 1297-1303). Cham:

Springer International Publishing.

Wang, W. (2007). *Autonomous control of a differential thrust micro rov* (Master's thesis, University of Waterloo).

Yılmaz, G., & Yılmaz, S. (2022). İnsansız Sualtı Araçlarında (İSA) Hidrodinamik Sürüklenme ve Kaldırma Kuvvetlerinin Derinlik ve Hıza Bağlı Değişiminin HAD ile Analizi. *International Journal of Engineering Research and Development*, *14*(1), 72-83.

Wang, S., Wang, L., Wang, J., & Chen, Y. (2024). Design and Structural Analysis of the ROV Framework Based on ANSYS. *Academic Journal of Engineering and Technology Science*, *7*(3).